PACS: 43.35.Yb, 61.05.cp, 61.66.Dk, 62.20.de, 81.05.X

V.M. Nadutov, O.I. Zaporozhets, N.A. Dordienko, V.A. Mikhaylovsky, S.Yu. Makarenko, A.V. Proshak

ULTRASONIC STUDY OF AS-CAST HETEROGENEOUS HIGH-ENTROPY ALLOY AlCuCrCoNiFe

G.V. Kurdyumov Institute for Metal Physics of N.A.S. of Ukraine, Kyiv, Ukraine

Received November, 11 2016

The longitudinal v_l and transverse v_t ultrasonic velocities in different geometric directions and sections of samples of as-cast equimolar high-entropy alloy (HEA) AlCuCrCoNiFe in spatially heterogeneous state are measured by means of the automated ultrasonic techniques of high resolution at the frequencies of 10–30 MHz. A considerable spread of the v_l and v_t values and the corresponding elastic moduli is revealed in different sections of samples. This fact points to spatial inhomogeneity of the HEA that is consistent with the existence of the α, γ_1 and γ_2 phases. Alongside with the spatial inhomogeneity, the anisotropy of ultrasonic velocities (4–8%) of the samples is revealed. The values of the elastic moduli $\langle E \rangle$, $\langle G \rangle$, $\langle B \rangle$, the Debye temperature Θ_D, the Poisson's ratio $\langle \eta \rangle$ and the ratio $\langle B \rangle / \langle G \rangle$ are calculated with using the averaged ultrasonic velocities $\langle v_l \rangle$, $\langle v_t \rangle$ and the mass density ρ. The acoustic parameters $\langle E \rangle$ = 199.1 GPa, $\langle G \rangle$ = 77.5 GPa, $\langle B \rangle$ = 159.9, $\langle \Theta_D \rangle$ = 498.4 K exceed those for pristine metals composing the HEA and indicate high interatomic bond stiffness, high resistance to dislocations movement and low compressibility. Relatively low established ratios $\langle \eta \rangle$ = 0.29 and $\langle B \rangle / \langle G \rangle$ = 2.132 are consistent with low plasticity of the HEA.

Keywords: as-cast high-entropy alloys, ultrasonic, elastic properties, inhomogeneities, elastic anisotropy

За допомогою автоматизованого ультразвукового методу високої роздільної здатності на частотах 10–30 MHz були виміряні поздовжня v_l і поперечна v_t швидкості ультразвуку в різних геометричних напрямках і на різних ділянках зразків у литому еквіатомному високоентропійному сплаві (ВЕС) AlCuCrCoNiFe в просторово неоднорідному стані. Виявлено значний розкид значень v_l і v_t та відповідних модулів пружності на різних ділянках зразків, що вказує на просторову неоднорідність ВЕС і узгоджується з існуванням α-, γ_1- і γ_2-фаз. Поряд з просторовою неоднорідністю виявлено анізотропію швидкостей ультразвуку (4–8%) у зразках. З використанням усереднених значень швидкостей ультразвуку $\langle v_l \rangle$, $\langle v_t \rangle$ і масової густини ρ розраховано величини модулів пружності $\langle E \rangle$, $\langle G \rangle$, $\langle B \rangle$, температури Дебая Θ_D, коефіцієнта Пуассона $\langle \eta \rangle$ і відношення $\langle B \rangle / \langle G \rangle$. Акустичні параметри $\langle E \rangle$ = 199.1 GPa, $\langle G \rangle$ = 77.5 GPa, $\langle B \rangle$ = 159.9, $\langle \Theta_D \rangle$ = 498.4 K перевищують ці значення для чистих металів, що входять до складу ВЕС, і вказують на високі жорсткість міжатомного зв'язку та високу стійкість до руху дислокацій і мале стис-

кання. Встановлено відносно низькі значення ⟨η⟩ = 0.29 і відношення ⟨B⟩/⟨G⟩ = 2.132, що узгоджується з низькою пластичністю ВЕС

Ключові слова: литий високоентропійний сплав, ультразвук, пружні властивості, неоднорідності, пружна анізотропія

1. Introduction

High-entropy alloys of the $Al_xCoCrCuFeNi$ system have attracted much attention during last 10 years due to their unusual structure and properties [1–7]. According to [1,2], the HEAs are characterized by large mixing entropy that means maximal chaos in atomic distribution. However, contrary to this statement, a number of experiments have shown that during crystallization, the majority of the HEAs are decomposed on dendrites and interdendrite zones and as-cast state contains two or more phases with simple crystal lattices: fcc, bcc, hcp [2–7].

The $Al_xCoCrCuFeNi$ HEA possess physical, mechanical and chemical properties which are widely covered in literature. The bcc phase increases hardness of the $Al_xCoCrCuFeNi$ HEA to 208–420 H_V depending on Al content [3,8]. High tensile mechanical properties of the as-cast $Al_xCrCuFeNiCo$ alloys are reported in [2,8,9] and complemented in [10,11]. High abrasive wear of the $Al_xCoCrCuFeNi$ ($0 \le x \le 3$) HEAs is reported in [8,12]. The HEA exhibits high thermal stability [2,11], the superior high-temperature strength sustained up to 800°C, enhanced plasticity and large work-hardening capability [8]. The strengthening mechanisms are considered in [2,11,13]. Thus the $Al_xCrCuFeNiCo$ HEA have a high potential for application as engineering materials in the tool-alloy and high-temperature alloy industry.

Important fundamental characteristics of a solid are elastic moduli, which determine mechanical properties. Particularly, the elastic moduli are needed for evaluation of the stress for dislocations movement, the fracture toughness, the work hardening rate as well as for estimation of the interatomic bond stiffness. At the same time, accurate information about elastic properties of the HEA is limited. The data upon the tensile Young's modulus [2,5] or the elastic modulus E obtained by means of indentation are mostly available [6,7,11]. However in these measurements, a probable elastic anisotropy of HEAs cannot be revealed.

The authors of [14] used dynamic-mechanical analyzer for measurement of the Young's modulus of the $Al_xCoCrFeNi$ (x = 0–1) alloys in the frequency range of 1–16 Hz. However the applied technique is an effective one to study internal friction in amplitude-dependent range and damping capacity of a material. Similar to other resonance techniques, this method is an integral one and it cannot test elastic properties of separate zones of a sample without its destruction. In [15], the elastic moduli of the equimolar CrMnCoFeNi HEA were measured in the temperature range of 50–300 K using the resonant ultrasound spectroscopy and sufficiently precise data upon weak temperature dependence of the Young's and the shear moduli were obtained. Notice that the alloy was Al-free and homogeneous single-phase (100% fcc) one.

Computer simulation by the EMTO-CPA calculation method was conducted and quantitative acoustic data were obtained in [16] for $Al_xHf_{1-x}NbTaTiZr$ HEA with respect to the concentration of Al and Hf. This approach was not applied to study the $Al_xCrCuFeNiCo$ HEAs although it has great potential for definition of elastic constants and its development could provide the basis for rapid ultrasonic test of texture in anisotropic HEAs.

Thus, there is insufficient experimental information upon precise quantitative elastic properties of the as-cast $Al_xCrCuFeNiCo$ HEAs, their spatial inhomogeneity and anisotropy. In this connection, the aim of this work was determination of acoustic and elastic properties of the as-cast equimolar AlCuCrCoNiFe HEA at room temperature with taking into account their heterogeneity and anisotropy.

For this purpose, the longitudinal v_l and transverse v_t ultrasonic velocities in various zones and in different geometric directions in a specimen of the AlCuCrCoNiFe alloy were measured by using automated ultrasonic equipment. Based on the obtained data, the bulk-wave ultrasonic velocities were averaged and the mass density ρ, the corresponding averaged elastic moduli $\langle E\rangle$, $\langle G\rangle$, $\langle B\rangle$, the ratio $\langle B\rangle/\langle G\rangle$, the Poisson's ratio $\langle\eta\rangle$ and the Debye temperature Θ_D were determined. At that special attention was paid to the extreme measured and calculated values giving the information upon spatial heterogeneity and anisotropy of the studied alloy.

2. Experimental details

The 1.2 kg ingots of the AlFeCoNiCuCr HEA were melted in the vacuum 10^{-5} torr induction furnace by melting of mixture of the elemental metals Al, Fe, Co, Ni, Cu, Cr with the purities of better than 99.9 wt%. The chemical composition of the alloy was determined by X-ray fluorescence analysis (Table 1). The X-ray diffractometer DRON-3M with the Co K_α-radiation was involved to characterize structure and phase composition of the AlFeCoNiCuCr HEA.

Table 1

Chemical composition of the AlFeCoNiCuCr HEA

Specimen	Elements, wt(at.)%					
	Al	Fe	Co	Ni	Cu	Cr
A_{1-2}, A'_{1-2}	9.3 (18.0)	18.2 (17.0)	18.2 (16.2)	19.0 (16.9)	19.47 (16.0)	15.7 (15.8)

The rectangular specimens (A_{1-2} and A'_{1-2}) with the dimensions of $6.146 \times 5.131 \times 5.025$ mm were machined for ultrasonic and X-ray diffraction experiments. The specimen planes were mechanically polished in order to attain their alignment for ultrasonic measurements. The deviation from the specified distances between parallel planes did not exceed ±2 μm. Samples of the denoted sizes were cut out from larger plates taking into account the results of scanning by

narrow ultrasonic beam. At that the most acoustically homogeneous areas were selected.

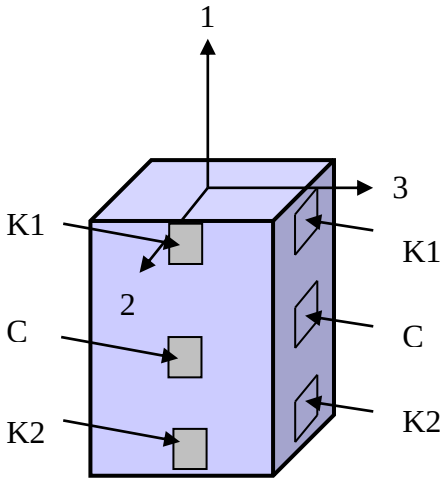

Fig. 1. Schematic view of a specimen for ultrasonic measurements

Fig. 1 represents a schematic view of a specimen in an orthogonal coordinate system where the symbols K1, C, K2 are the zones of the specimen tested by sonic.

The ultrasonic measurements were executed on frequencies of 10–30 MHz at $T = 20 \pm 1$°C by automated techniques described in [17,18]. The bulk-wave ultrasonic velocities v_{ij} were measured in the K1, C, K2 zones of a specimen in three orthogonal directions (Fig. 1). The first index of v_{ij} corresponds to the direction of ultrasonic wave propagation and the second one corresponds to the orientation of polarization vector. In addition, the selective automatic scanning of a specimen along direction 1 at the orientation of the wave vector of the longitudinal ultrasonic wave in directions 2 (v_{22}) or 3 (v_{33}) was carried out. The size of the beam cross-section for longitudinal and transverse waves did not exceed 2 and 4 mm, respectively.

Ultrasonic velocity was measured upon the time interval of passing through a zero value of identical periods of high-frequency filling of a selected pair of the reflected ultrasonic pulses. The absolute instrumental error of measurement of the v_{ij} on a time base of 10 μs was 10^{-4}, and the relative error was by one order less. The real error of the ultrasonic velocities in the studied objects was estimated upon spread of the measured values. The density ρ of specimens was measured using quartz as etalon by means of the differential Archimedes' method with the error of 10^{-4} on 10 g specimen. Procedures for measurement and analysis of experimental data were carried out by using appropriate software. The calculations of the elastic parameters and the Debye temperature were performed by using well known expressions:

$$G = \rho \langle v_t \rangle^2, \tag{1}$$

$$E = GA, \tag{2}$$

$$B = GA/3(3 - A), \tag{3}$$

$$\eta = (a^2 - 2)/2(a^2 - 1), \tag{4}$$

$$B/G = A/3(3 - A), \tag{5}$$

$$A = (3a^2 - 4)/(a^2 - 1), \tag{6}$$

$$\Theta_D = \frac{h}{k}\left(\frac{9N\rho}{4\pi A_\Sigma}\right)^{1/3}\left(\frac{1}{\langle v_l\rangle^3}+\frac{1}{\langle v_t\rangle^3}\right)^{-1/3}, \qquad (7)$$

where $a = \langle v_l\rangle / \langle v_t\rangle$; $\langle v_l\rangle$ and $\langle v_t\rangle$ are the averaged bulk ultrasonic velocities; h is the Planck's constant; k is the Boltzmann constant; N is the Avogadro number; A_Σ is the total atomic weight. It could be noted that the ratio B/G as well as the Poisson's ratio η characterizes plasticity of metals and alloys [19].

3. Results and discussion

Table 2 represents the measured longitudinal ultrasonic velocity v_{ii} in different zones (Fig. 1, K1, C, K2) in orthogonal directions of a specimen of the as-cast AlFeCoNiCuCr HEA, its averaged values in each orthogonal directions, the anisotropy of the v_{ii}. The analogous data for transverse ultrasonic velocity v_{ij} are represented in Table 3.

Table 2

The values of the longitudinal ultrasonic velocity v_{ii} in different zones (K1, C, K2) of a specimen in orthogonal directions of the as-cast AlFeCoNiCuCr HEA, the averaged values of v_{ii} in each directions 1, 2, 3, the magnitude of the ultrasonic velocity anisotropy ($An_{3–2}$, $An_{3–1}$, $An_{1–2}$) and its maximal relative dispersion. The values of An_{3j}, An_{2j} were obtained by rotating of the polarization vector of the transverse waves in a plain perpendicular to the wave vector. X, $\langle X\rangle$, $\Delta X_{max}/\langle X\rangle$ are the generalized denotations of the ultrasonic values

Specimen	X	Zone of specimen			$\langle X\rangle$	$\Delta X_{max}/\langle X\rangle$, %
		K1	C	K2		
$A_{1–2}$	v_{33}, m/s	6074.4	6096.2	6142.2	6104.3	1.11
	v_{22}, m/s	6048.7	5988.7	5907.5	5981.6	2.36
	v_{11},m/s	–	6192.3	–	6192.3	–
	$An_{3–2}$, %	0.04	1.76	3.89	2.03	–
	$An_{3–1}$, %	–	1.58	–	1.43	–
	$An_{1–2}$, %	–	3.34	–	3.46	–
$A'_{1–2}$	v_{33}, m/s	6078.2	6054.6	6026.4	6053.1	0.86
	v_{22}, m/s	6029.5	6118.3	6095.6	6081.1	1.46
	v_{11}, m/s	–	6034.9	–	6034.9	–
	$An_{3–2}$, %	0.80	1.05	1.14	0.46	–
	$An_{3–1}$, %	–	0.03	–	0.30	–
	$An_{1–2}$, %	–	1.37	–	0.76	–

It is evident from the Table 2 that the maximum of anisotropy of longitudinal velocity An_{3-2} = 3.89% is observed in the $A_{1–2}$ specimen towards to 3 direction on

specimen edge in zone K1. For the sample A'_{1-2} in zone K2 $An_{3\text{-}2}$ = 1.14%. The maximum spread of the v_{ii} values is also small (2.36 and 1.46% for specimens A_{1-2} and A'_{1-2}, respectively). Anisotropy of the transverse velocity is observed in the same directions. The spread of the v_{ij} values attains 4.91% (specimen A_{1-2}) and 7.52% (specimen A'_{1-2}), respectively (Table 3).

Table 3

The transverse ultrasonic velocity v_{ij} in different zones (K1, C, K2) of a specimen of the as-cast AlFeCoNiCuCr HEA, the averaged values of v_{ij} ($\langle v_{21,23}\rangle$, $\langle v_{31,32}\rangle$), its anisotropy (An_{31-32}, An_{21-23}) and averaged values in orthogonal directions 2 and 3

Specimen	X	Zone of specimen			$\langle X\rangle$	$\Delta X_{max}/\langle X\rangle$, %
		K1	C	K2		
A_{1-2}	v_{31}, m/s	3424.3	3462.9	3490.4	3459.2	1.91
	v_{32}, m/s	3596.7	3596.7	3486.5	3560.0	3.10
	$\langle v_{31,32}\rangle$, m/s	3510.5	3529.8	3488.4	3509.6	1.18
	An_{31-32}, %	4.91	3.79	0.11	2.94	4.91
	v_{21}, m/s	3493.1	3516.1	3539.9	3513.0	1.33
	v_{23}, m/s	3568.7	3525.9	3492.6	3529.1	2.16
	$\langle v_{21,23}\rangle$, m/s	3530.9	3521.0	3516.2	3522.7	0.42
	An_{21-23}, %	2.14	0.28	1.34	1.25	2.14
	$\langle v_{12,13}\rangle$, m/s	–	3423.9	–	3423.9	–
A'_{1-2}	v_{31}, m/s	3595.6	3653.4	3453.7	3567.6	5.60
	v_{32}, m/s	3547.7	3549.9	3558.5	3552.0	0.30
	$\langle v_{31,32}\rangle$, m/s	3571.6	3601.6	3506.1	3559.8	2.68
	An_{31-32}, %	1.34	2.87	2.99	2.40	2.99
	v_{21}, m/s	3559.4	3429.0	3454.2	3480.9	3.75
	v_{23}, m/s	3688.3	3696.9	3595.9	3660.4	2.76
	$\langle v_{21,23}\rangle$, m/s	3623.8	3562.9	3495.0	3560.6	3.62
	An_{21-23}, %	3.56	7.52	2.34	4.47	7.52
	$\langle v_{12,13}\rangle$, m/s	–	3401.8	–	3401.8	–

Table 4 represents the results of the generalization of the data presented in Table 2 and Table 3 for the as-cast AlFeCoNiCuCr HEA.

Table 4

The ratio of the longitudinal velocity and the averaged transverse velocity $v_{ii}/\langle v_{ij,ik}\rangle$, the maximal dispersion of the ratio $v_{ii}/\langle v_{ij,ik}\rangle$, its averaged values and maximal dispersion in a direction, the resulting average values of the ultrasonic velocities $\langle v_l\rangle$ and $\langle v_t\rangle$ and their ratio $a = \langle v_l\rangle/\langle v_t\rangle$ for specimens of the as-cast AlFeCoNiCuCr HEA

Specimen	X	Zone of specimen			$\langle X\rangle$	$\Delta X_{\max}/\langle X\rangle$, %
		K1	C	K2		
A_{1-2}	$v_{33}/\langle v_{31,32}\rangle$	1.730	1.727	1.761	1.739	1.96
	$v_{22}/\langle v_{21,23}\rangle$	1.713	1.701	1.680	1.698	1.94
	$v_{11}/\langle v_{12,13}\rangle$	–	1.809	–	1.809	–
	$\langle v_l\rangle$, m/s	–	–	–	6092.7	–
	$\langle v_t\rangle$, m/s	–	–	–	3503.0	–
	$\langle v_l\rangle/\langle v_t\rangle$	–	–	–	1.739	–
A'_{1-2}	$v_{33}/\langle v_{31,32}\rangle$	1.702	1.681	1.719	1.701	2.23
	$v_{22}/\langle v_{21,23}\rangle$	1.664	1.717	1.744	1.708	4.68
	$v_{11}/\langle v_{12,13}\rangle$	–	1.809	–	1.809	–
	$\langle v_l\rangle$, m/s	–	–	–	6056.4	–
	$\langle v_t\rangle$, m/s	–	–	–	3537.3	–
	$\langle v_l\rangle/\langle v_t\rangle$	–	–	–	1.712	–

It is evident from the Table 4 that along with a slight dispersion $\Delta X_{\max}/\langle X\rangle$ of the averaged ultrasonic velocities $\langle v_{21,23}\rangle$ (0.42% for the sample A_{1-2} and 3.62% for the sample A'_{1-2}) the ratio $\langle v_{ii}\rangle/\langle v_{ij}\rangle$ in different zones of a plane of specimen A_{1-2} does not exceed 2% and of specimen A'_{1-2} attains 4.68%.

The investigated specimens were scanned in direction 1 by the longitudinal ultrasonic beam with the wave vectors 2 or 3 (Fig. 1). The corresponding dependences $v_{22}(x)$, $E_2(x)$ and $v_{33}(x)$, $E_3(x)$ were calculated taking into account the relative constancy of the $v_l/v_t(x)$. Fig. 2 represents typical scan results by the longitudinal ultrasonic beam for velocity $v_{33}(x)$ and modulus $E_3(x)$ of both A_{1-2} and A'_{1-2} specimens. In this case the Young's modulus $E_3(x)$ vs. coordinate x in 3rd direction is plotted upon the $v_{33}(x)$ dependence. It is evident that the dependencies $E_3(x)$ for both samples show similar behavior. The values of the longitudinal ultrasonic velocity and the Young's modulus are varied within the intervals 6004–6124 m/s and 218–231 GPa, respectively (Fig. 2). Similar behavior was observed for share modulus and bulk modulus.

Using the data presented in Table 4 the averaged bulk ultrasonic velocities $\langle v_l\rangle$, $\langle v_t\rangle$, the averaged elastic moduli $\langle E\rangle$, $\langle G\rangle$, $\langle B\rangle$, the ratio $\langle B\rangle/\langle G\rangle$, the Poisson's ratio

⟨η⟩ and the Debye temperature Θ_D of the as-cast AlFeCoNiCuCr HEA were calculated and shown in Table 5.

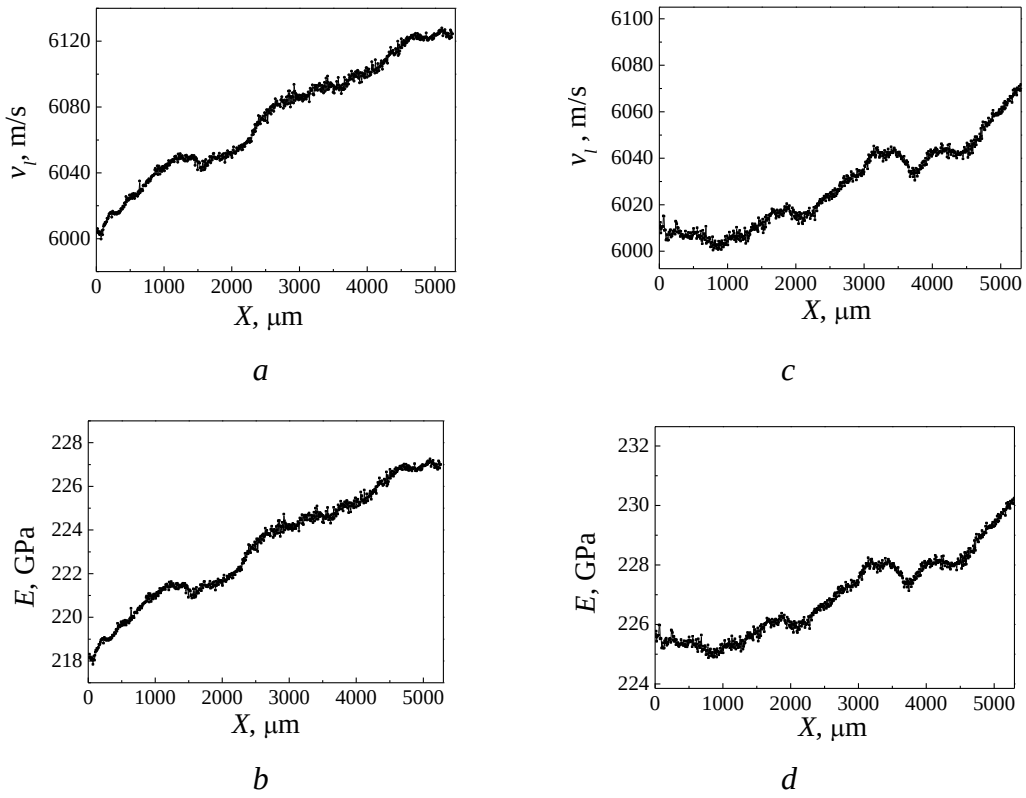

Fig. 2. Typical curves of scan from K1 to K2 zones (Fig. 1) with the longitudinal ultrasonic beam of a specimen of the AlFeCoNiCuCr HEA: *a*, *b* are the specimen $A_{1–2}$; *c*, *d* are the specimen $A'_{1–2}$; *a*, *c* are the ultrasonic velocity $v_{33}(X)$ in 3rd direction; *b*, *d* are the Young's modulus in 3rd direction $E_3(X)$. The ratios $v_l/v_t = a_1 = 1.739$ for the specimen $A_{1–2}$ and $v_l/v_t = a_2 = 1.701$ for the specimen $A'_{1–2}$ (Table 4)

The calculated elastic parameters show variation of the values depending on the minimal and maximal ultrasonic velocities derived from the same plain of the sample (Table 5). In particular the Young's modulus ⟨*E*⟩ of the as-cast AlFeCoNiCuCr HEA is varied within the range of 173.4–226.9 GPa. The bulk modulus ⟨*B*⟩ and the shear modulus ⟨*G*⟩ have values 146.1–168.0 and 65.3–91.4 GPa, respectively.

Thus the anisotropy of acoustic and elastic parameters and their big dispersion were revealed in the as-cast equimolar AlFeCoNiCuCr HEA. The cause of the anisotropic behavior is dendrite microstructure combined with chemical inhomogeneity of the as-cast state. First of all it is well-established inhomogeneous distribution of chemical elements [5,20–22] and the presence of the specific dendrites microstructure of the as-cast alloy (Fig. 3).

Micrograph of the as-cast HEA AlCuCoFeNiCr exhibits existence of gray dendritic creations (D) with the average size of 150–200 μm (Fig. 3, arrow 1), dark

Table 5

The values of mass density ρ, the acoustic and elastic parameters of the as-cast AlFeCoNiCuCr HEA calculated with using maximal, minimal and averaged v_l and v_t values

	Specimen			
	$A_{1–2}$	$A'_{1–2}$	$A_{1–2}$	$A_{1–2}$
ρ, g/cm^3	7.309	7.305	7.309	7.309
$\langle v_l \rangle$, m/s	6092.7	6056.4	5907.5	6000.1
$\langle v_t \rangle$, m/s	3503.0	3537.3	2988.7	3245.9
$\langle E \rangle$, GPa	224.8	226.9	173.4	199.1
$\langle G \rangle$, GPa	89.7	91.4	65.3	77.5
$\langle B \rangle$, GPa	151.7	146.1	168.0	159.9
$\langle B \rangle / \langle G \rangle$	1.691	1.598	2.574	2.132
$\langle \eta \rangle$	0.253	0.241	0.328	0.290
Θ_D, K	508.0	512.2	488.8	498.4
Note	Max values of v_l and v_t		Min values of v_l and v_t	Averaged values of v_l and v_t

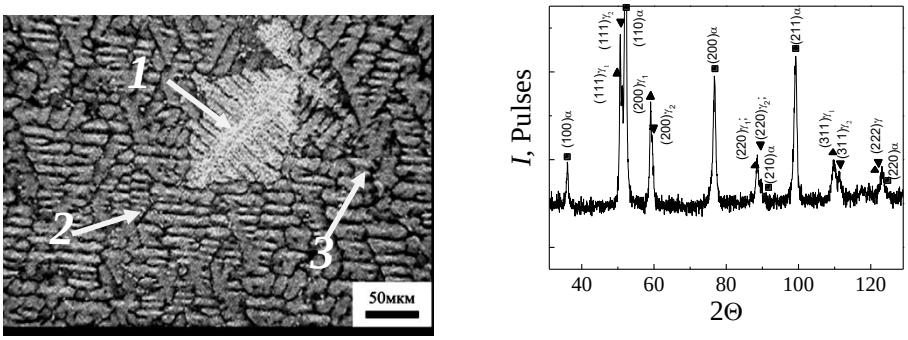

Fig. 3. Microstructure of the as-cast HEA AlCuCoFeNiCr: *1* is the denrite axis; *2* is the ID zone; *3* is the inclusion enriched with Cu [20]

Fig. 4. XRD powder diffractograms of the as-cast AlFeCoNiCuCr HEA ($A_{1–2}$). XRD pattern for $A'_{1–2}$ is similar

interdendritic zones (ID) (arrow 2) with white inclusions (arrow 3). According to [20], the D branches and ID zones are formed from mutually dissolved elements of corresponding concentrations whereas a fraction of excessive elements with low temperature of crystallization (for example Cu) is displaced into ID zones. In fact an essential inhomogeneous distribution of Cu in the as-cast HEA AlCuCoFeNiCr with its prevailing localization in ID zones was revealed in [5,20].

Besides, XRD analysis has revealed three phases in the as-cast AlFeCoNiCuCr HEA: one bcc phase α and two fcc phases γ_1 and γ_2 (Fig. 4,*a*,*b*) that is consistent with the data reported in [3–5]. According to the electron microscopy studies [6,7]

the as-cast HEAs contain even more nanosized phases with different morphology, structure (A2, B2, $L1_2$) and chemical composition. The lattice parameter of the bcc phase is a_α = 0.2879 nm and of the fcc phases are $a_{\gamma 1}$ = 0.3629 nm and $a_{\gamma 2}$ = 0.3599 nm. The ratio of the phases 26 : 12 : 62 is estimated using the ratio of the integral intensities $I\gamma_1 : I\gamma_2 : I\alpha$ of the $(111)\gamma_1$, $(111)\gamma_2$ and $(110)\alpha$ diffraction lines taking into account the multiplicity factors relating to fcc and bcc lattices.

Consequently the as-cast equimolar AlFeCoNiCuCr HEA is a heterogeneous material with the complex structure, phase composition and distribution of chemical elements and the precise ultrasonic techniques and proposed approach provide its express testing.

The obtained averaged elastic moduli and the Debye temperature have high values $\langle E \rangle$ = 199.1 GPa, $\langle \Theta_D \rangle$ = 498.4 K (Table 5) in the most part of specimens in our precise experiment. Particularly the Young's modulus is higher than that measured in tensile experiment on the $Al_xFeCoNiCr$ HEA (x = 1) 163 GPa [2] and estimated by indentation of the AlFeCoNiCr HEA 168 GPa [23]. In addition it is reported in [5–7], the tensile and indented Young's modulus of the equimolar AlCoCrCuFeNi alloy does not exceed 180–182 GPa. This difference between dynamical ultrasonic data and mechanically testing ones is usually observed for the majority of alloys.

The increased Young's modulus and the Debye temperature of the as-cast AlFeCoNiCuCr HEA (Table 5) is a good evidence of the high interatomic bond stiffness. This is consistent with the strong binding effect in HEA mentioned in [2]. The high bulk modulus $\langle B \rangle$ = 159.9 GPa means weak compressibility of the HEA.

On the other hand, relatively large share modulus $\langle G \rangle$ = 77.5 GPa means high resistance to dislocations movement in the HEA. Moreover the ratio $\langle B \rangle / \langle G \rangle$ = 2.132 is low as compared to pristine Al 2.93–3.08; Cu 2.76–2.90; Co 2.32 [24] and Cr 2.27 [25] and higher than that for pristine Fe 1.99 and Ni 2.02 (Table 5). These data along with the relatively low Poisson's ratio indicate low plasticity of the HEA at room temperature. This is consistent with high hardness [3,8,20] and tensile mechanical properties of the as-cast $Al_xCoCrCuFeNi$ HEAs [2,8–11].

Notice that estimation of the elastic moduli of the HEAs upon ultrasonic measurements data requires obligatory taking into account anisotropy of the acoustic parameters, which can be associated with the oriented dendritic microstructure.

4. Conclusions

1. The as-cast equimolar AlCuCrCoNiFe HEA is elastically inhomogeneous and anisotropic system. Anisotropy of longitudinal ultrasonic velocity v_l attains 4% and of transverse ultrasonic velocity v_t achieves 7.5–8% resulting from oriented dendritic microstructure.

2. The averaged values of the elastic moduli $\langle E \rangle$ = 199. GPa, $\langle G \rangle$ = 77.5 GPa, $\langle B \rangle$ = 159.9 GPa and the Debye temperature $\langle \Theta_D \rangle$ = 498.4 K of the HEA exceed those for pristine metals composing this alloy and indicate high interatomic bond stiffness, high resistance to dislocations movement and low compressibility. The relatively low values of the Poisson's ratio $\langle \eta \rangle$ = 0.29 and the ratio $\langle B \rangle / \langle G \rangle$ = 2.132 are consistent to the low plasticity of the HEA.

3. The obtained results are evidences of a suitability of the applied ultrasonic technique for diagnostics of elastic properties and related characteristics of the inhomogeneous HEAs. The obtained results will be used for improvement of technology to manufacturing of HEAs with more homogeneous structure.

This work was carried out with financial support of the Project 22/15-H within the Target Complex Program of N.A.S. of Ukraine «Fundamental Problems of the Creation of New Nanomaterials and Nanotechnologies» and partially of the budget program 022/15-B of the Structure and Properties of Solid Solution Department of the G.V. Kurdyumov IMP of N.A.S. of Ukraine. Authors express thankful to V.P. Zalutskii for X-Ray measurements.

1. *S. Ranganathan*, Curr. Sci. **85**, 1404 (2003).
2. *J.W. Yeh, S.K. Chen, S.J. Lin, J.Y. Gan, T.S. Chin, T.T. Shun, C.H. Tsau, S.Y. Chang*, Adv. Eng. Mater. **6**, 299 (2004).
3. *C.C. Tung, J.W. Yeh, T.T. Shun, S.K. Chen, Y.S. Huang, H.C. Chen*, Mater. Lett. **61**, 1 (2007).
4. *C.J. Tong, Y.L. Chen, S.K. Chen, J.W. Yeh, T.T. Shun, C.H. Tsau, S.J. Lin, S.Y. Chang*, Metall. Mater. Trans. **A36**, 881 (2005).
5. *S. Singh, N. Wanderka, B.S. Murty, U. Glatzel, J. Banhart*, Acta Mater. **59**, 182 (2011).
6. *M.V. Ivchenko, V.G. Pushyn, N. Wanderka*, Journal Technical Physics **84**, 57 (2014).
7. *M.V. Ivchenko, V.G. Pushyn, A.N. Uksusnikova, N. Wanderka*, Phys. Metals Metallography **114**, 561 (2013).
8. *C.J. Tong, Y.L. Chen, S.K. Chen, J.W. Yeh, T.T. Shun, C.H. Tsau, S.J. Lin, S.Y. Chang*, Metall. Mater. Trans. **A36**, 1263 (2005).
9. *K.Y. Tsai, M.H. Tsai, J.W. Yeh, C.C. Yang*, J. Alloys Compd. **490**, 160 (2010).
10. *A.V. Kuznetsov, G.A. Salishchev, O.N. Senkov, N.D. Stepanov, D.G. Shaysultanov*, Belgorod State University Scientific bulletin, Series: Mathematics. Physics **27**, 191 (2012).
11. *S.A. Firstov, V.F. Gorban, N.A. Krapivka, E.P. Pechkovsky, N.I. Danilenko, M.V. Karpets*, Modern problems of physical material **18**, 140 (2009).
12. *J.M. Wu, S.J. Lin, J.W. Yeh, S.K. Chen, Y.S. Huang, H.C. Chen*, Wear **261**, 513 (2006).
13. *Y.P. Wang, B.S. Li, H.Z. Fu*, Adv. Eng. Mater. **8**, 641 (2009).
14. *S.G. Ma, P.K. Liaw, M.C. Gao, J.W. Qiao, Z.H. Wang, Y. Zhang*, J. Alloys Compd. **604**, 331 (2014).

15. *A. Haglund, M. Koehler, D. Catoor, E.P. George, V. Keppens*, Intermetallics **58**, 62 (2015).
16. *S. Li, X. Ni, F. Tian*, Coatings **5**, 366 (2015).
17. *A.S. Osipov, S. Nauyoks, T.W. Zebra, O.I. Zaporozhets*, Diamond and Related Materials **18**, 1061 (2009).
18. *O.I. Zaporozhets, S.A. Kotrechko, N.A. Dordienko, V.A. Mykhailovsky, A.V. Zatsarnaya*, Problems of atomic science and technology № 2, 197 (2015).
19. *S.F. Pugh*, Philosophical Magazine **367**, 823 (1954).
20. *V.M. Nadutov, S.Yu. Makarenko, P.Yu. Volosevich, V.P. Zalutskii*, Metallofizika i Noveishie Tekhnologii **36**, 1327 (2014).
21. *V.M. Nadutov, S.Yu. Makarenko, P.Yu. Volosevich*, Phys. Metals Metallography **116**, 439 (2015).
22. *V.M. Nadutov, A.V. Proshak, S.Yu. Makarenko, V.Ye. Panarin, M.Ye. Svavil'nyj*, Mater. Sci. Technology **47**, № 2–3, 272 (2016).
23. *S.A. Firstov, S.T. Mileyko, V.F. Gorban, N.A. Krapivka, E.P. Pechkovsky*, Composites and Nanostructures **6**, 125 (2014).
24. *W.P. Mason*, Physical Acoustics: Principles and Methods, Academic press, New York and London (1965).
25. *I.N. Franzevytch, F.F. Voronov, C.A. Bakuta*, Elastic constants and elastic moduli of metals and nonmetals, Naukova Dumka, Kiev (1982).

В.М. Надутов, О.И. Запорожец, М.А. Дордиенко, В.А. Михайловский, С.Ю. Макаренко, А.В. Прошак

УЛЬТРАЗВУКОВЫЕ ИССЛЕДОВАНИЯ ЛИТОГО НЕОДНОРОДНОГО ВЫСОКОЭНТРОПИЙНОГО СПЛАВА AlCuCrCoNiFe

С помощью автоматизированного ультразвукового метода высокого разрешения на частотах 10–30 MHz измерены продольная v_l и поперечная v_t скорости ультразвука в различных геометрических направлениях и на разных участках образцов в литом эквиатомном высокоэнтропийном сплаве (ВЭС) AlCuCrCoNiFe в пространственно неоднородном состоянии. Обнаружен значительный разброс значений v_l и v_t и соответствующих модулей упругости на различных участках образцов, что указывает на пространственную неоднородность ВЭС и согласуется с существованием α-, γ_1- и γ_2-фаз. Наряду с пространственной неоднородностью выявлена анизотропия ультразвуковых скоростей (4–8%) в образцах. С использованием усредненных скоростей ультразвука $\langle v_l \rangle$, $\langle v_t \rangle$ и массовой плотности ρ рассчитаны значения модулей упругости $\langle E \rangle$, $\langle G \rangle$, $\langle B \rangle$, температура Дебая Θ_D, коэффициент Пуассона $\langle \eta \rangle$ и отношение $\langle B \rangle / \langle G \rangle$. Акустические параметры $\langle E \rangle$ = 199.1 GPa, $\langle G \rangle$ = 77.5 GPa, $\langle B \rangle$ = 159.9, $\langle \Theta_D \rangle$ = 498.4 K превышают эти значения для чистых металлов, входящих в состав ВЭС, и указывают на высокие жесткость межатомной связи и устойчивость к движению дислокаций и малую сжимаемость. Установлены относительно низкие значения $\langle \eta \rangle$ = 0.29 и отношения $\langle B \rangle / \langle G \rangle$ = 2.132, что согласуется с низкой пластичностью ВЭС

Ключевые слова: литой высокоэнтропийный сплав, ультразвук, упругие свойства, неоднородности, упругая анизотропия